Magnetohydrodynamic Phenomena in Galaxies, Accretion Disks and Star Forming Regions@Chiba Univ. 05.11.18

Three-dimensional MHD Simulations of Jets from Accretion Disks

Hiromitsu Kigure & Kazunari Shibata

ApJ in press (astro-ph/0508388)

Basic Properties of the Jets (1)

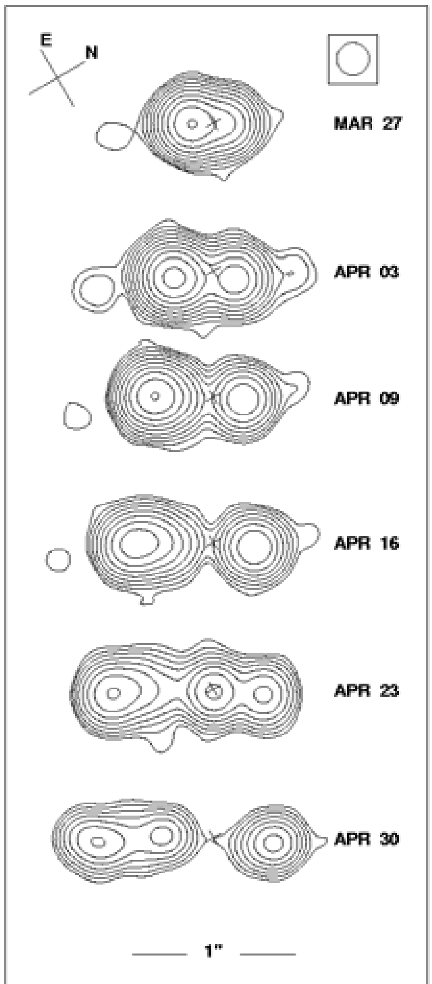

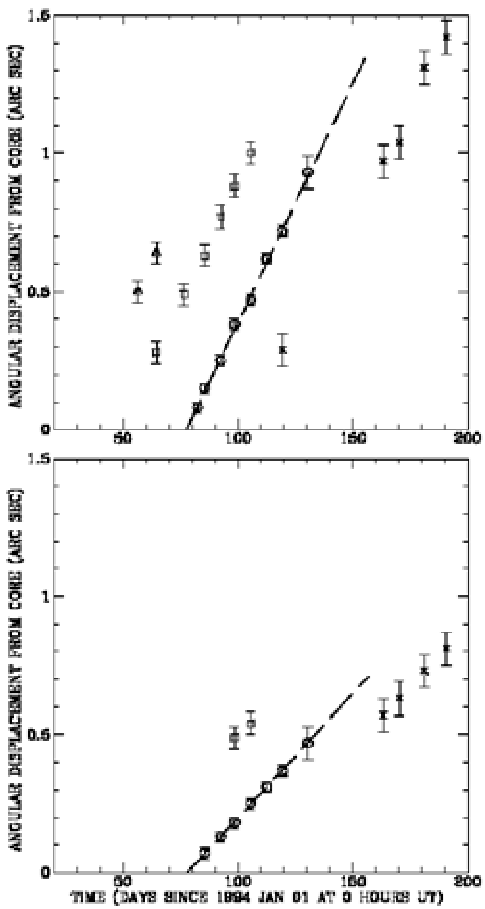

1. <u>Relativistic velocity up to ~ c</u>

   The velocity is almost equal to the escape velocity of the central object.

Consistent with the MHD model (see, e.g., Shibata & Uchida 1986, Kudoh, Matsumoto, & Shibata 1998).

GRS1915+105

Mirabel & Rodriguez 1994
Rodriguez & Mirabel 1999

Basic Properties of the Jets (2)

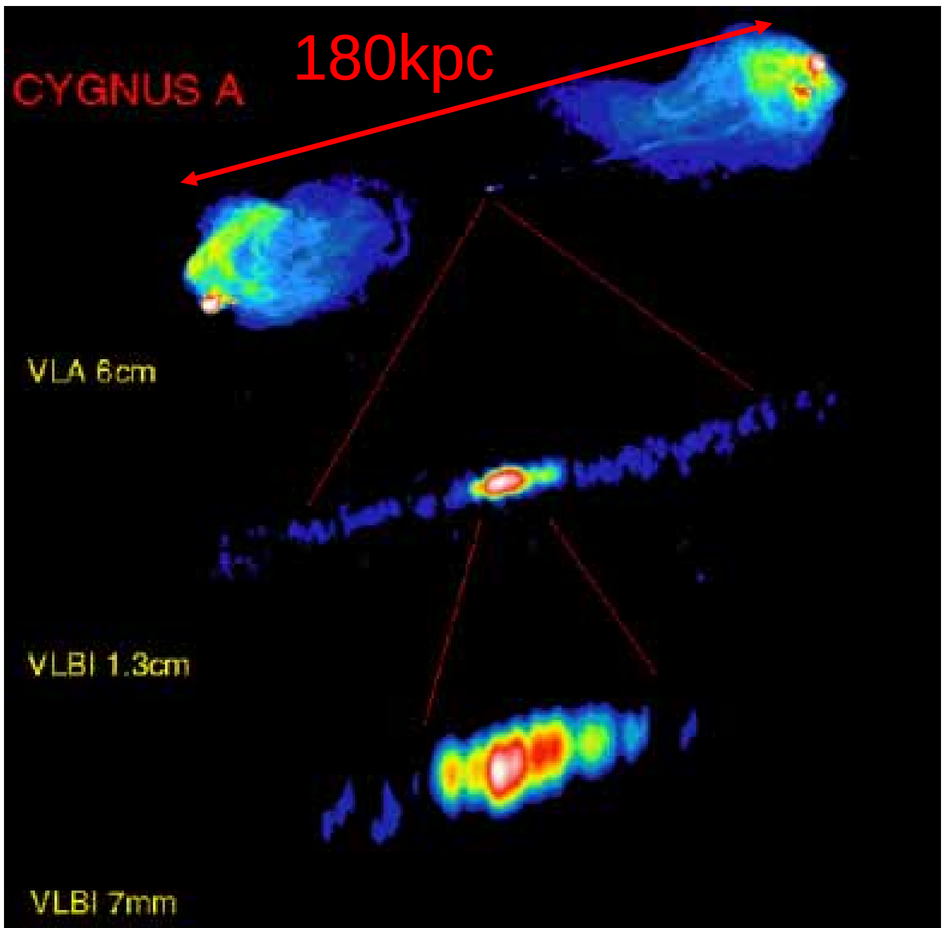

2. The jets extend over kpc to Mpc, keeping its collimation.

<u>The jets must be capable of exceptional stability.</u>

How about the stability of MHD jet?

Motivation of Our Research

The mechanisms of the jet launching from the accretion disk and the collimation: Shibata & Uchida 1986, Matsumoto et al. 1996, Kudoh et al. 1998 (2.5-D axisymmetric simulations).

The stability of the propagating jet (beam) injected as the boundary condition in 3-D: Hardee & Rosen (1999, 2002), Ouyed, Clarke, & Pudritz (2003)

In our research, it is investigated whether the MHD jets launched from the accretions disk are stable in 3-D, by solving the interaction of the magnetic field and the accretion disk.

Basic Equations

Ideal MHD Equations

$$\frac{\partial \rho}{\partial t} + \boldsymbol{v} \cdot \nabla \rho = -\rho \nabla \cdot \boldsymbol{v}$$

$$\frac{\partial \boldsymbol{v}}{\partial t} + \boldsymbol{v} \cdot \nabla \boldsymbol{v} = -\frac{1}{\rho} \nabla \left(p + \frac{\boldsymbol{B}^2}{8\pi} \right) + \frac{1}{4\pi\rho} \boldsymbol{B} \cdot \nabla \boldsymbol{B} + \boldsymbol{g}$$

$$\frac{\partial p}{\partial t} + \boldsymbol{v} \cdot \nabla p = -\gamma p \nabla \cdot \boldsymbol{v}$$

The calculation scheme is CIP-MOC-CT.

$$\frac{\partial \boldsymbol{B}}{\partial t} + \nabla \times \boldsymbol{E} = 0$$

$$\boldsymbol{E} = -\boldsymbol{v} \times \boldsymbol{B}$$

I developed the 3-D cylindrical code by myself. The number of grid points is (N_r, N_ϕ, N_z) = (171, 32, 195).

CIP-MOC-CT Scheme

CIP: A kind of Semi-Lagrange method. Using the CIP for solving the hydro-part of the equations. 3rd order interpolation with the physical value and its derivative. Therefore, the time evolution of the derivatives is also calculated (see, e.g., Kudoh, Matsumoto, & Shibata 1999).

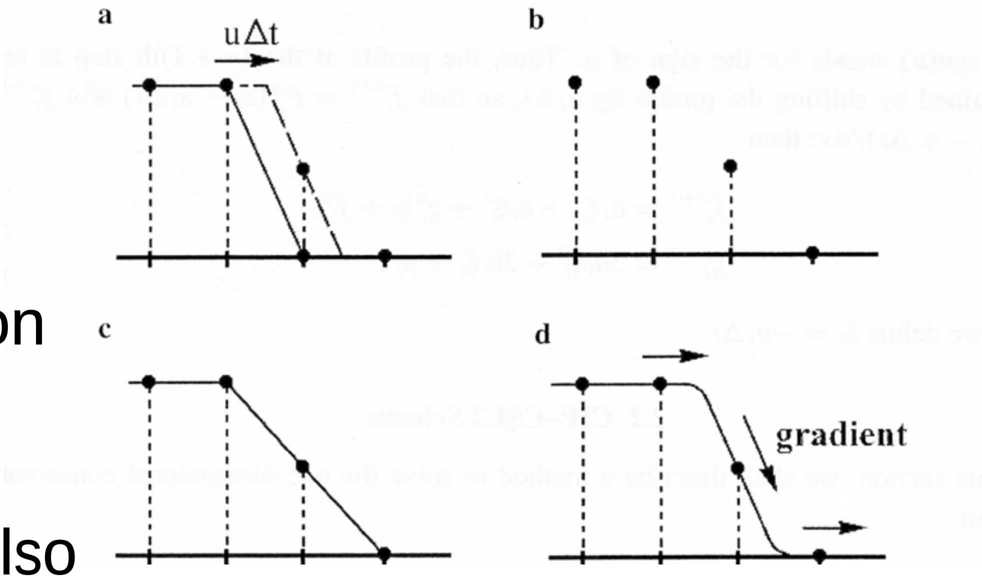

MOC：The accurate method solving the propagation of the liner Alfven waves.

CT：Solving the induction equation with the constraint of divB=0.

Initial Condition (1)

Accretion disk: an rotation disk in equilibrium with the point-mass gravity, centrifugal force, and the pressure gradient force.

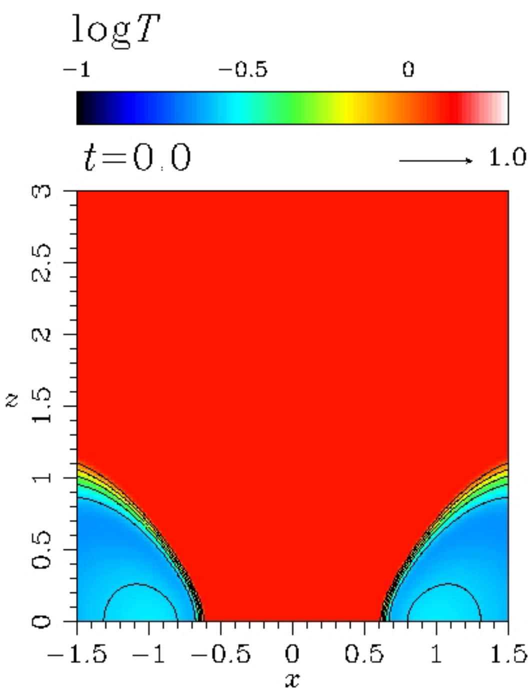

Initial magnetic field: a vertical and uniform large-scale magnetic field. The ratio of the magnetic to gravitational energy, $E_{mg} = (V_{A0}{}^2 / V_{K0}{}^2)$, is the parameter for the initial magnetic field strength.

The typical value is $E_{mg} = 5.0 \times 10^{-4}$.
The plasma-**β** in the disk～200, **β** in the corona～4.

Initial Condition (2)

Nonaxisymmetric perturbation: the amplitude is the 10% of the sound velocity at (r,z)=(1.0,0.0), and with the form of

1. sin2**φ** (sinusoidal)
2. random number between –1 and 1 instead of sinusoidal function (random)

E_{mg}: 8 parameters

24 runs in total (including the no perturbation cases).

E_{mg}	Perturbation		
	Nothing	Sinusoidal	Random
1.0×10^{-5}	A1	S1	R1
2.0×10^{-5}	A2	S2	R2
5.0×10^{-5}	A3	S3	R3
1.0×10^{-4}	A4	S4	R4
2.0×10^{-4}	A5	S5	R5
5.0×10^{-4}	A6	S6	R6
1.0×10^{-3}	A7	S7	R7
2.0×10^{-2}	A8	S8	R8

Time Evolution

Axisymmetric

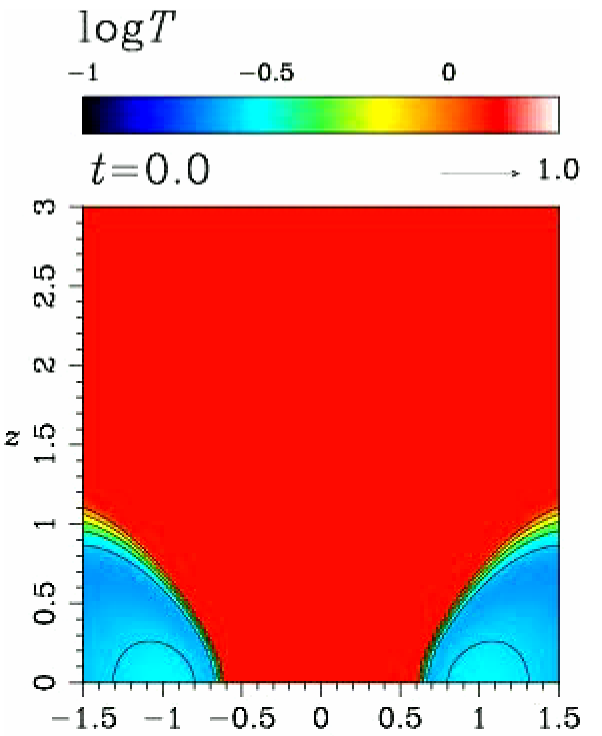

Sinusoidal

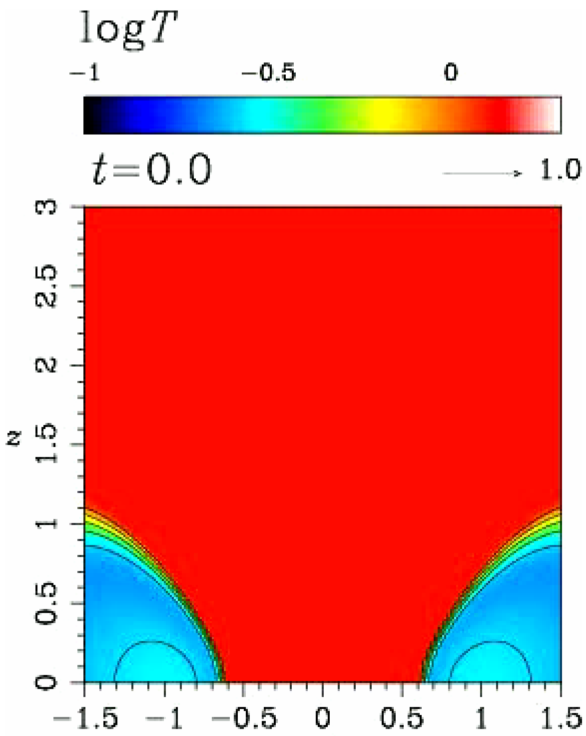

Random

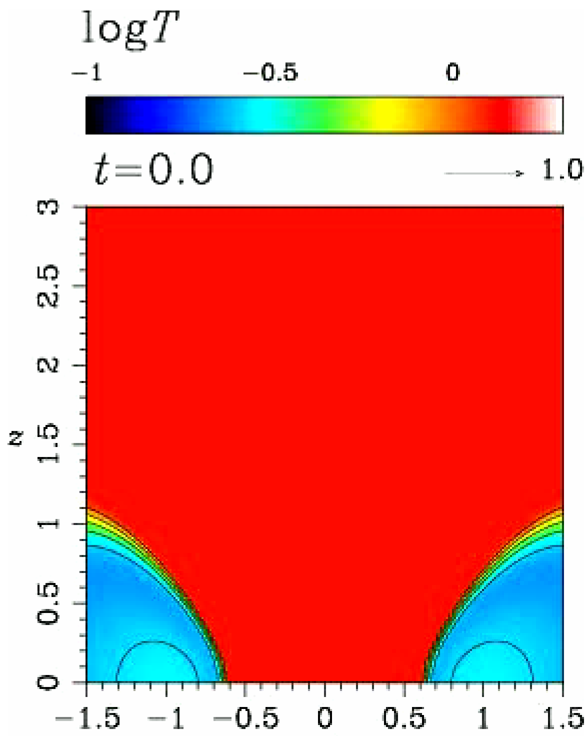

On the x-z plane

3D movie

Nonaxisymmetric in the Jet

The slice on this plane.

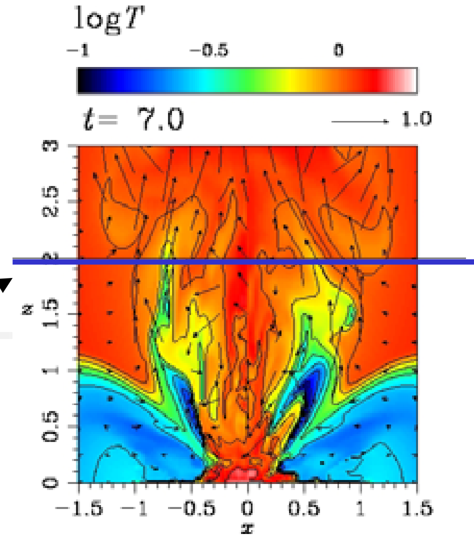

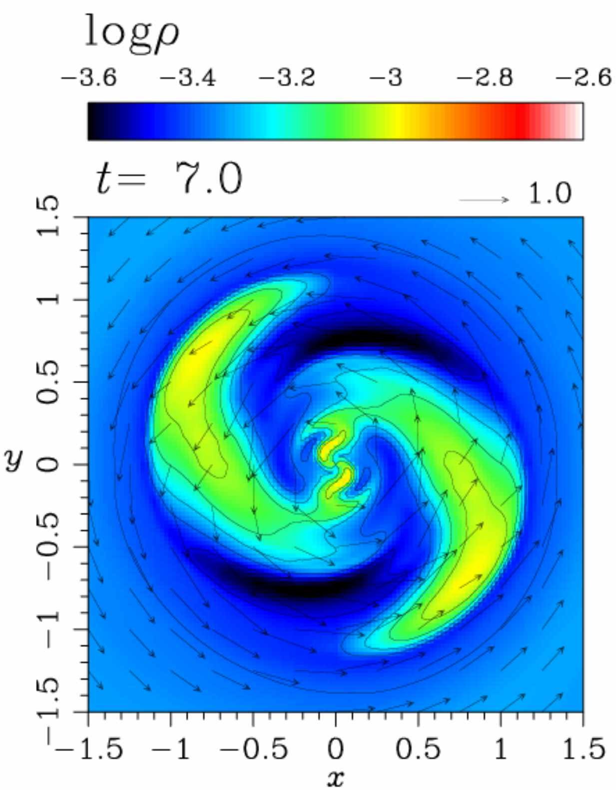

Model S6

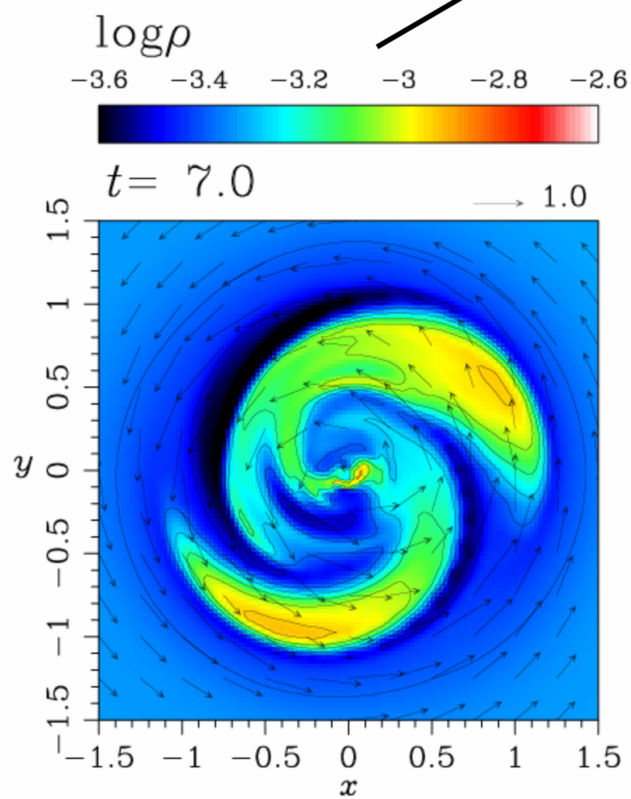

Model R6

The jets seem to have the non-axisymmetric structure with m=2 even in the random perturbation case.

Power Spectra in the Jet and Disk (1)

Time evolution of the Fourier power spectra of the non-axisymmetric modes of the magnetic energy.

$$\tilde{E}_M\left(k_r, m, k_z\right) = \frac{1}{V_s} \iiint_{V_s} E_M\left(r, \phi, z\right) e^{i(k_r r + m\phi + k_z z)} r dr d\phi dz$$

Then, integrate about k_r, k_z.

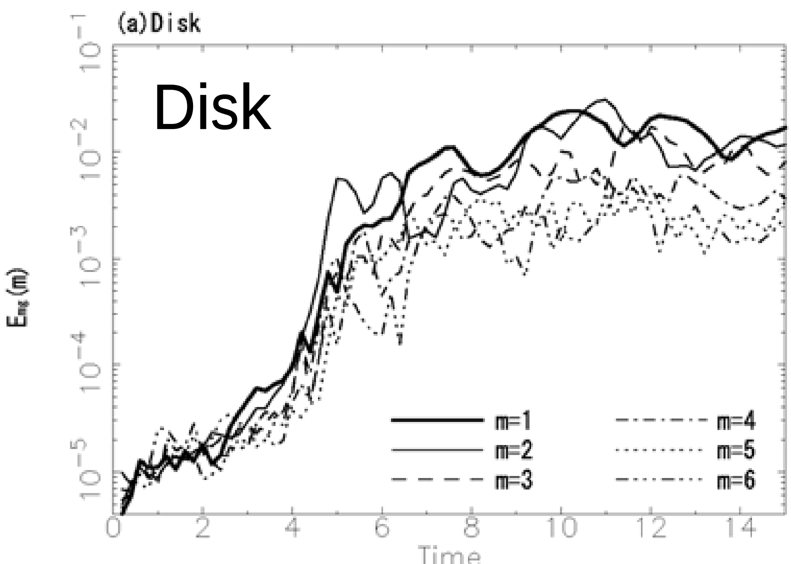

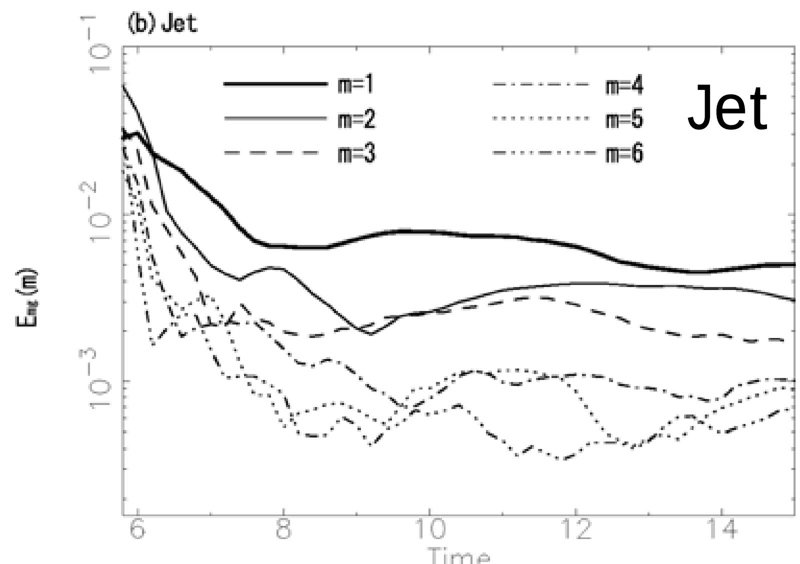

Power Spectra in the Jet and Disk (2)

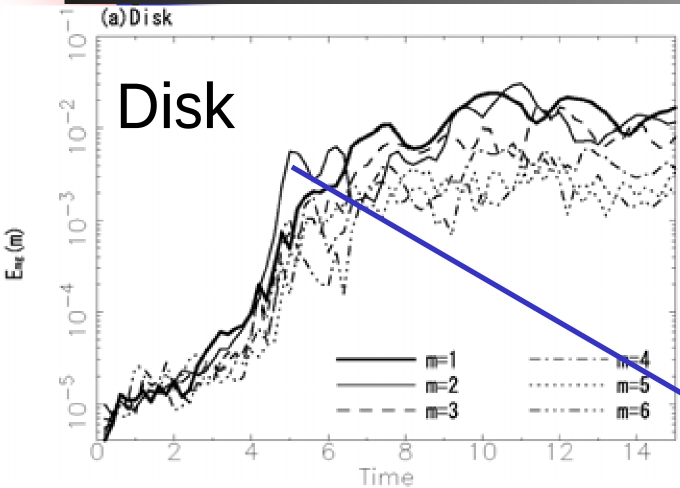

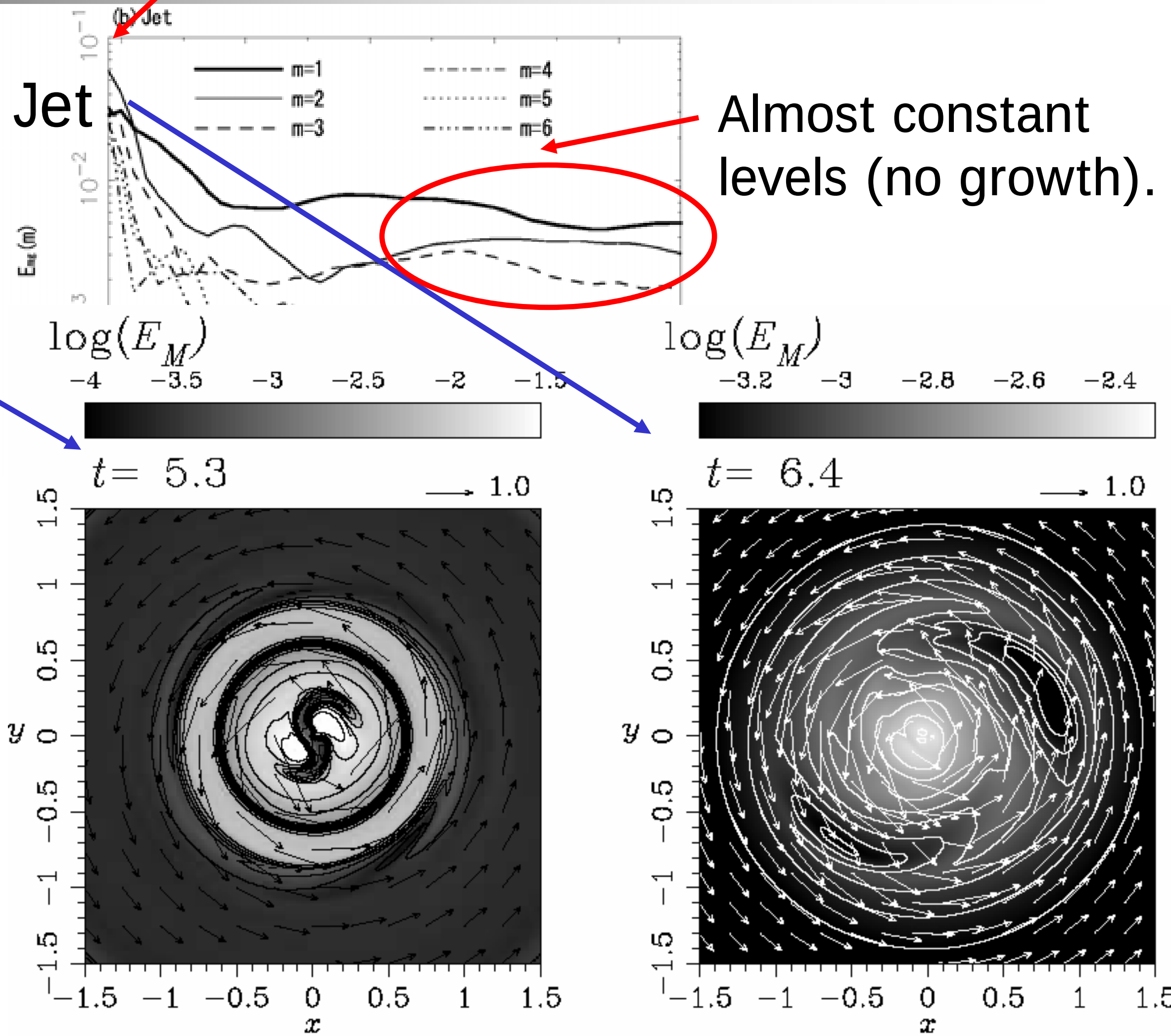

The flare-up of the m=2 mode spectrum in the disk before the dominance of the m=2 mode in the jet.

Growth Rate of Nonaxisymmetric Modes of MRI

MRI: Magneto-Rotational Instability

$$\frac{k^2}{k_z^2}\left[\frac{d^2}{dt^2}+(\boldsymbol{k}\cdot\boldsymbol{v}_A)^2\right]^2\delta B_R+\left[\kappa^2+6\,\frac{m^2}{k_z^2R^2}\left(\frac{d\Omega}{d\ln R}\right)^2\right]\left[\frac{d^2}{dt^2}+(\boldsymbol{k}\cdot\boldsymbol{v}_A)^2\right]\delta B_R$$
$$-\left[1+\frac{m^2}{k_z^2R^2}\left(\frac{d\ln\Omega}{d\ln R}\right)^2\right]4\Omega^2(\boldsymbol{k}\cdot\boldsymbol{v}_A)^2\delta B_R-6\,\frac{mk_R}{k_z^2R}\,\frac{d\Omega}{d\ln R}\left[\frac{d^2}{dt^2}+(\boldsymbol{k}\cdot\boldsymbol{v}_A)^2\right]\frac{d\delta B_R}{dt}=0$$

Balbus & Hawley 1992、Eq. (2.24)

Solving this dispersion relation numerically, the growth rate of the m=2 mode is **ω**=0.54 (detailed parameters).

exp[**ω**t]=5.1（t=3.0）. On the other hand, the power spectrum of the m=2 mode became 5.9 times larger than the initial value (reference).

Amplification of the Magnetic Field in the Disk (1)

MRI→Amplification of the magnetic energy

Check differences between the models.

Total
Inner region (r<0.6)
Outer region (r>0.6)

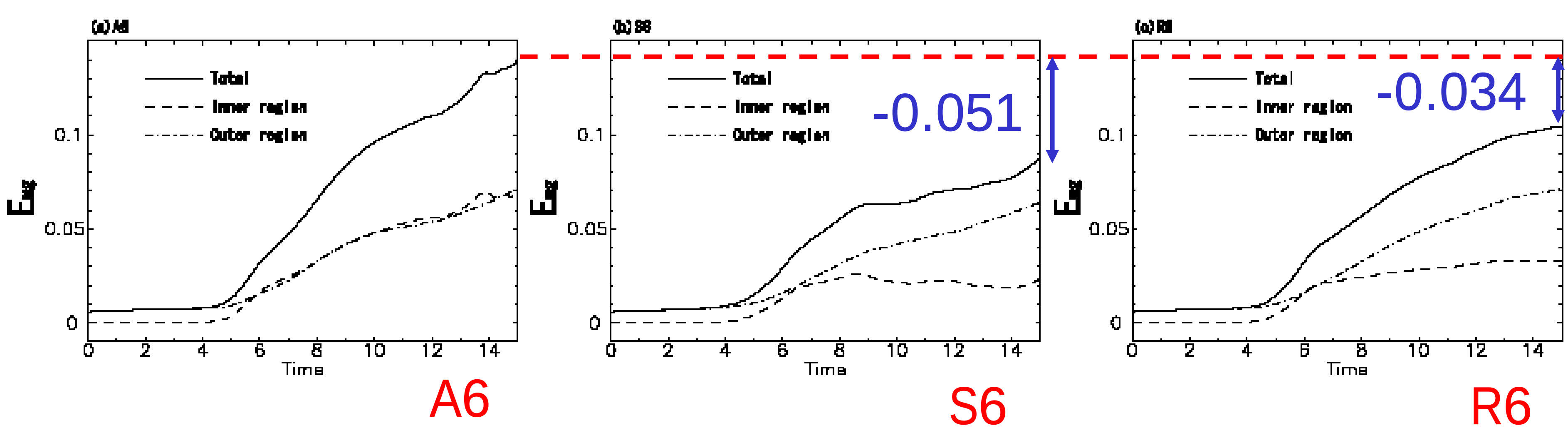

Outer region: No significant difference among the models.

Inner region: Significant difference between the models.

Amplification of the Magnetic Field in the Disk (2)

$$\frac{\partial}{\partial t}\left(\frac{B^2}{8\pi}\right) = -\underline{\boldsymbol{v}\cdot(\boldsymbol{J}\times\boldsymbol{B})} - \underline{\frac{1}{4\pi}\nabla\cdot(\boldsymbol{E}\times\boldsymbol{B})}$$

The work done by the Lorentz force.

Poynting flux

$$\frac{\partial}{\partial t}\left\langle\frac{B^2}{8\pi}\right\rangle = -\underbrace{\langle\mathbf{v}\cdot(\mathbf{J}\times\mathbf{B})\rangle}_{①} - \underbrace{\frac{1}{4\pi}\int(\mathbf{E}\times\mathbf{B})\cdot d\mathbf{S}}_{②}$$

<>: Volume integral

Color function

Amplification of the Magnetic Field in the Disk (3)

The minus sign: kinetic → magnetic energy

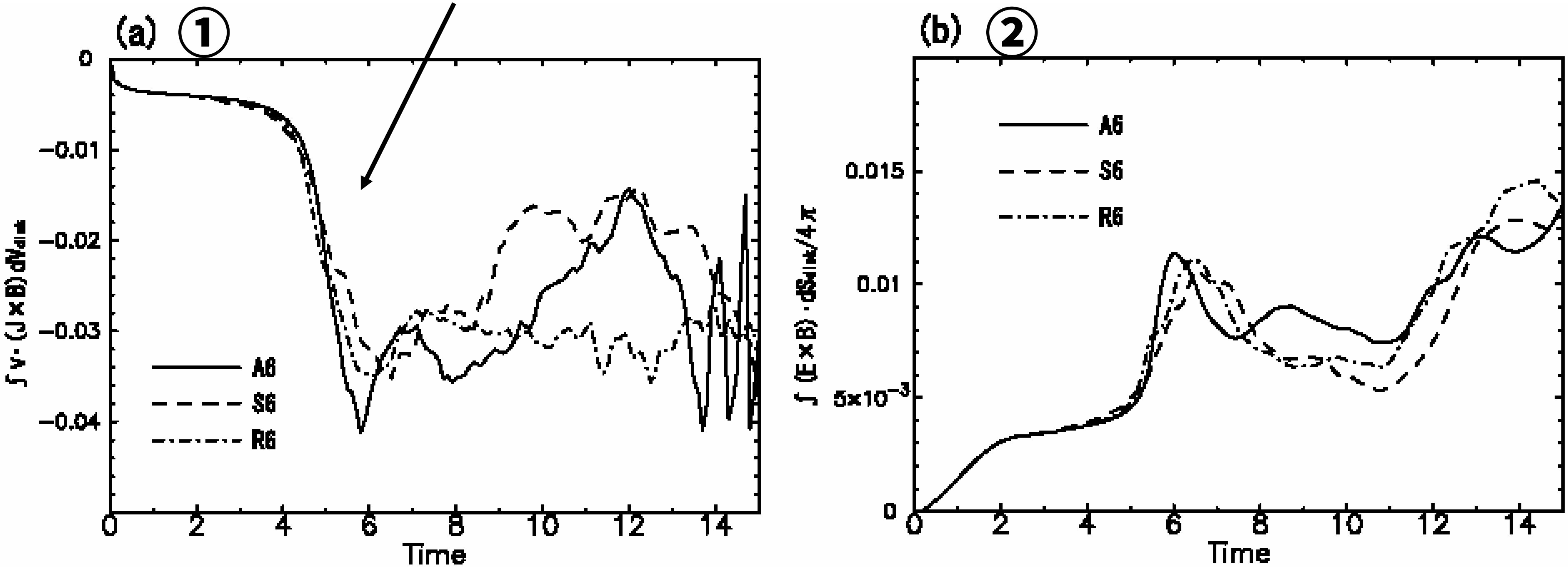

The sum of the time integration of ① and ② = increase of E_{mg}

→The difference between models A6 and S6 is consistent.

Not consistent between A6 and R6→Numerical Reconnection.

Angular Momentum Transport (1)

The mass accretion is important for the activity of AGNs, not limited to the jet formation.

↓

How does it extract the angular momentum of the disk?
→ **α** -disk model: assumption of the viscosity parameter.

Recently, it has been cleared that the magnetic turbulence is the origin of the viscosity.

How large is the amount of the extracted angular momentum in the radial direction? How about in the axial (z) direction?

The symbol “<< >>” means the spatial and temporal average.

Angular Momentum Transport (2)

E_{mg}	$\langle\langle -\frac{B_r B_\phi}{4\pi}\rangle / \langle p\rangle\rangle^{\rm d}$ (5)	$\langle\langle -\frac{B_\phi B_z}{4\pi}\rangle / \langle p\rangle\rangle$ (6)	$\langle\langle -\frac{B_r B_\phi}{4\pi}\rangle / \langle p\rangle\rangle^{\rm d}$ (5)	$\langle\langle -\frac{B_\phi B_z}{4\pi}\rangle / \langle p\rangle\rangle$ (6)
1.0×10^{-5}	0.0035	0.0068	0.0041	0.0056
2.0×10^{-5}	0.0079	0.012	0.0090	0.010
5.0×10^{-5}	0.018	0.022	0.021	0.020
1.0×10^{-4}	0.030	0.032	0.033	0.031
2.0×10^{-4}	0.051	0.044	0.048	0.045
5.0×10^{-4}	0.089	0.063	0.079	0.067
1.0×10^{-3}	0.14	0.082	0.12	0.084
2.0×10^{-3}	0.17	0.093	0.14	0.10
	Axisymmetric		Random	

Over a wide range of E_{mg}, the efficiencies of the angular momentum transport in the radial and axial directions are comparable.

Comparison with Steady Theory and Nonsteady Axisymmetric Simulation

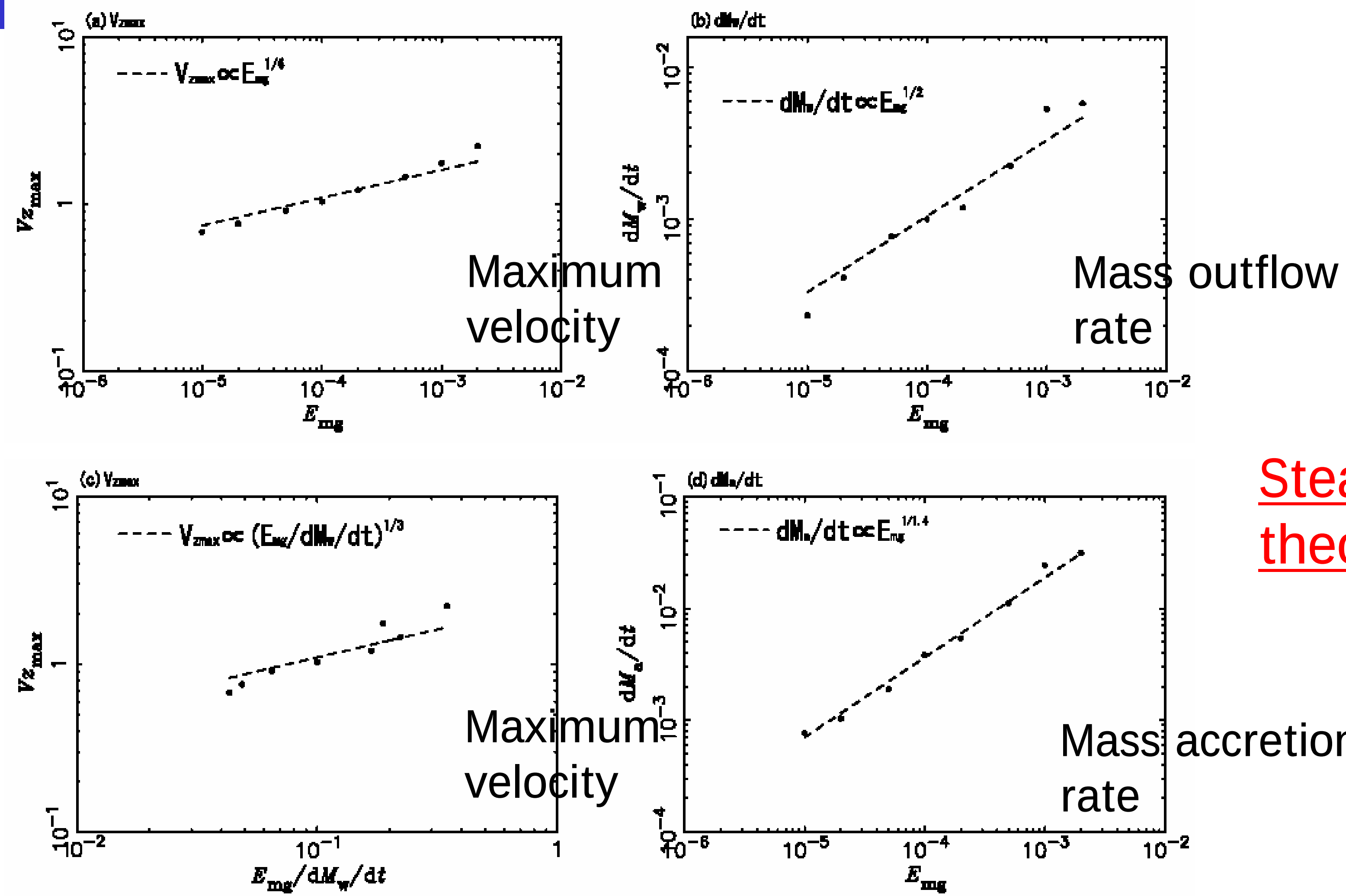

<u>Steady theory</u>

Summary (1)

1. The jet launched from the accretion disk is stable, at least for 2.5 orbital periods of the accretion disk (there is no indication for the disturbance to grow).

2. The nonaxisymmetric disturbance made in the accretion disk owing to magnetorotational instability (MRI) propagates into the jet.

3. It is suggested that, in the random perturbation case, the magnetic field is complexly twisted and the numerical reconnection takes place in the inner region of the disk. We need to perform the resistive simulation in the future.

Summary (2)

3. The efficiency of the angular momentum transport does not depend on the model (the type of the initial perturbation). The efficiencies in the radial (r) and axial (z) direction are comparable in the wide range of initial magnetic field strength.

4. Though the jet has the nonaxisymmetric structure, the macroscopic properties (e.g., the maximum jet velocity) are almost the same as those in the axisymmetric case shown by Kudoh et al. (1998).

Parameters for Solving the Dispersion Relation

Alfven velocity: V_A=0.056 from the initial condition.

Radial wavelength: λ_r=0.4 from the spatial distribution of E_{mg}.

Radial position: R=1.0

Axial wavelength: λ_z=0.35 (~$2\pi V_A/\Omega$: most unstable λ).

Angular velocity: Ω=1.0 (angular velocity at R=1.0)

Epicyclic frequency: κ=0.0 (constant angular momentum disk).

Return

Growth of the Spectrum in the Disk

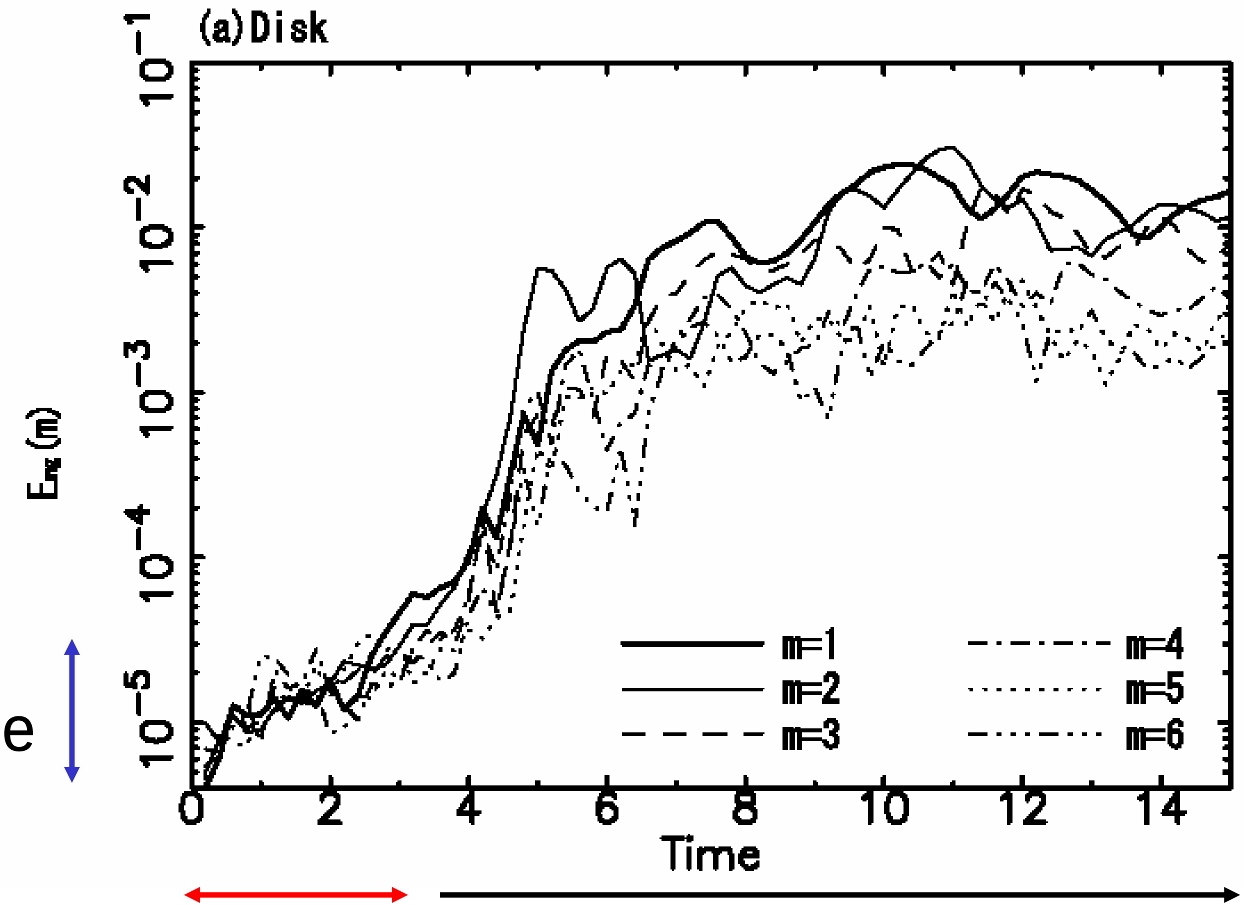

Increase by the factor of 5.9.

Linear growth Nonlinear growth

Return

Color Function

Color function Θ. Initially,

$$\Theta = \begin{cases} 1 & \text{inside of the disk} \\ 0 & \text{outside of the disk} \end{cases}$$

Calculating the time evolution of Θ by

$$\frac{d\Theta}{dt} = \frac{\partial\Theta}{\partial t} + v_r \frac{\partial\Theta}{\partial r} + \frac{v_\phi}{r}\frac{\partial\Theta}{\partial\phi} + v_z \frac{\partial\Theta}{\partial z} = 0$$

The region where Θ is not equal to zero is the extent to which the matter originally in the disk reaches.

Return

Steady Theory (1)

$$v_{\infty} \approx \frac{B}{\sqrt{4\pi\rho}}$$

The terminal velocity of the jet is comparable to the Alfven velocity (magnetically accelerated).

$$\frac{v_{\varphi} - r\Omega}{v_p} = \frac{B_{\varphi}}{B_p}$$

Seen from the corotating frame with the magnetic field, the velocity and magnetic fields are parallel (frozen-in condition).

Steady Theory (2)

At the infinity ($r \sim \infty$), $V_\phi \sim 0$ because the angular momentum is finite.

$$-\frac{r\Omega}{v_\infty} = \frac{B_\varphi}{B_p} \qquad r \sim \infty:\ B_\phi/B_p >> 1 \longrightarrow \qquad v_\infty \approx \frac{B_\varphi}{\sqrt{4\pi\rho}}$$

The mass outflow rate is expressed as $\dot{M} = 4\pi r^2 \rho v_\infty$

$$v_\infty{}^2 = \frac{r^2 v_\infty B_\varphi{}^2}{\dot{M}} = \frac{r^4 \Omega^2 B_p{}^2}{\dot{M}} \rightarrow v_\infty = \left(\frac{\Omega^2 B_p{}^2 r^4}{\dot{M}} \right)^{1/3}$$

Steady Theory (3)

$$\dot{M} \propto \begin{cases} B_p^{\ 0} & \text{: Strong initial magnetic field case } (B \sim B_p >> B_\phi). \\ B_p^{\ 1} & \text{: Weak initial magnetic field case } (B \sim B_\phi >> B_p). \end{cases}$$

See, e.g., Kudoh & Shibata 1995

Eventually,

$$v_\infty \propto \begin{cases} B_p^{\ 2/3} \\ B_p^{\ 1/3} \end{cases}$$

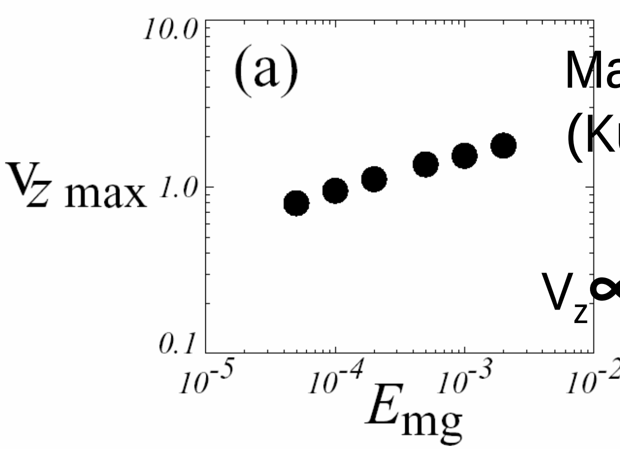

Maximum jet velocity (Kudoh et al. 1998).

$V_z \propto E_{mg}^{\ 1/6} \propto B_p^{\ 1/3}$

Steady Theory (4)

Steady theory

$$\dot{M} \propto \begin{cases} B_p^{\,0} \\ B_p^{\,1} \end{cases}$$

$$v_\infty = \left(\frac{\Omega^2 B_p^{\,2} r^4}{\dot{M}} \right)^{1/3}$$

Michel’s solution

Nonsteady Simulations

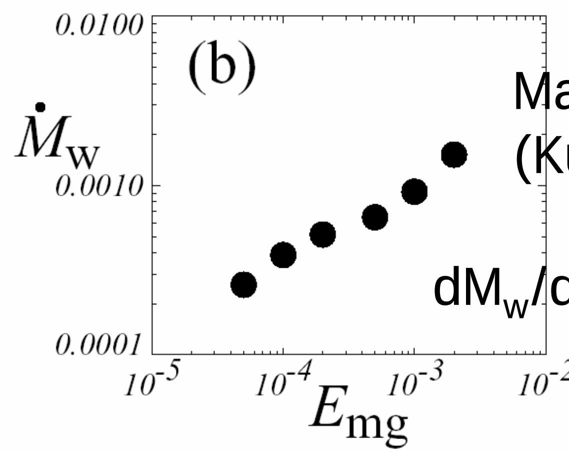

Mass accretion rate (Kudoh et al. 1998)

$dM_w/dt \propto E_{mg}^{1/2} \propto B_p^{1}$

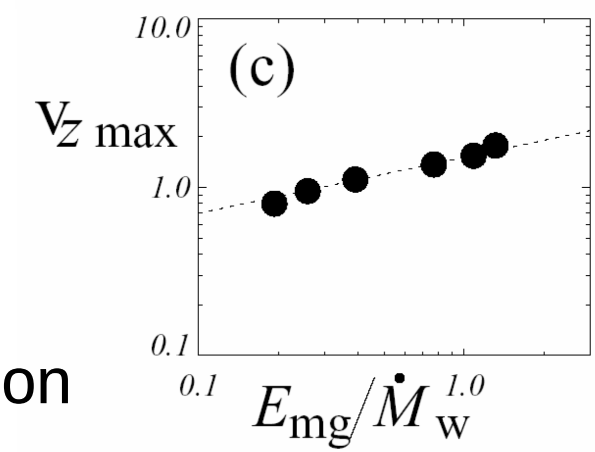

Return